FOUR-DIMENSIONAL PHASE UNWRAPPING ALGORITHM FOR RETRIEVING EARTHQUAKE DISPLACEMENT FROM SENTINEL-1A SATELLITE

Maged Marghany and Shattri Mansor
Geospatial Information Science Research
Centre, Faculty of Engineering
University Putra Malaysia
43400 UPM, Serdang, Selangor
Email :magedupm@hotmail.com

KEYWORDS: Sentinel-1A satellite, Nepal earthquake, Hybrid Genetic Algorithm, 4-D best-path avoiding singularity loops, Decorrelation, Interferogram.

ABSTRACT:
This study utilizes 4-D phase unwrapping technique to retrieve earthquake displacement due to Nepal earthquake, 2015. In doing so, the hybrid genetic algorithm is implemented to optimize 4-D phase unwrapping algorithm based on fourth-dimensional best-path avoiding singularity loops (4DBPASL) algorithm. The algorithm modification from 3-D to 4-D has implemented prior to hybrid genetic algorithm. The study shows 4DBPASL can present the interferogram from 2-D to 4-D. The study also shows that 4DBPASL able to reconstruct 2-D earthquake displacement into 4-D view. In conclusion, 4DBPASL algorithm can be used to produce accurate 4-D quake deformation using Sentinel-1A satellite.

1. INTRODUCTION

Since the 1800s, the fourth Dimension are scrutinized by Scientists, Psychologists, Philosophers, Mathematicians and Physicists. Indeed, scientists have implemented 4-D concepts to explicate roughly of the universe. At early stage, scientists created 4-D from 3-D by spinning 3-D about its image or itself. Scientists therefore, have deliberated the time as a dimension beside the 3-D. Nevertheless, this theory scientifically is not precise. The fourth Dimension axis *which goes through the Z,Y and Z* . The 4D object has four fundamental unite: width ,length heights and 4-D which is *W* . A hypercube, for instance, has a length, width, height and a fourth dimension that is perpendicular to all three of the other units. In other words, 4-D is exploring the inner objects of 3-D. In remote sensing satellite-based interferometric synthetic aperture radar (InSAR) is a potential tool for precise measurements of 3-D ground shifts triggered off by earthquakes or landslides. At present, the elevation models that are available for large parts of Earth are of low resolution, inconsistent or incomplete. Scientists addressed temporal, geometric and atmospheric decorrelations are most critical limitations (Pepe 2012; Marghany 2012; Marghany 2014a). Consistent with Zebker et al., (1997), short temporal baseline, appropriate spatial baseline, decent weather circumstances and ascending and descending SAR data are consistent criteria to restrain decorrelation and noise to produce a reliable DEM. ERS-1 and ERS-2, Terara X-SAR in tandem mode are the excellent example of short temporal resolution.

In wide range of contexts, TanDEM-X and TerraSAR-X are imaging the terrain below them simultaneously, from different angles Marghany (2014b). These images are processed into precise elevation maps with a 12 m resolution and any vertical accuracy better than 2 m. Image coregistration, InSAR an interferometric phase estimation (or noise filtering) and interferometric phase unwrapping (Zebker et al., 1997; Hussien 2005; Marghany 2012) are three keys processing procedures of InSAR. It is well known that the performance of interferometric phase estimation suffers seriously from poor image coregistration. Interferogram filtering algorithms such as adaptive contoured window, pivoting mean filtering, pivoting median filtering, and adaptive phase noise filtering are the main methods for the conventional InSAR interferometric phase estimation (Pepe 2012). Recently, Pepe (2012) stated that DinSAR has recently applied with success to investigate the temporal evolution of the detected deformation phenomena through the generation of displacement time-series. In this context, two main categories of advanced DInSAR techniques for deformation time-series generation have been proposed in literature, often referred to as Persistent Scatterers (PS); and small Baseline (SB) techniques, respectively. The PS algorithms select all the interferometric data pairs with reference to a single common master image, without any constraint on the temporal and spatial separation (baseline) among the orbits.

However, the two-dimensional unwrapping methods could introduce discontinuous regions when the noise is high. The resulting inconsistent baselines within a slice would produce an incorrectly unwrapped baseline. Then the one-dimensional baseline unwrapping could give incorrect results. Many of the methods apply to quality map to guide

the unwrapping procedures. The quality map was defined with the quality of the edges that connects two neighboring voxels and unwrap the most reliable voxels first (Marghany 2013). Therefore, three-dimensional phase unwrapping approach, which considers the temporal domain and the spatial domain restrictions simultaneously (Marghany 2014a). The main contribution of this study is to combine Hybrid Genetic Algorithm (HGA) with 4-D phase unwrapping algorithm of 4-D best-path avoiding singularity loops (4-DBPASL) algorithm with InSAR technique. Two hypotheses examined are: (i) the HGA algorithm can be used as filtering technique to reduce noise in the 4-D phase unwrapping; and (ii) 4-D Nepal earthquake displacement can be reconstructed using satisfactory phase unwrapping of 4DBPASL by involving HGA optimization algorithm.

2. STUDY AREA

Gorkha earthquake is most horrible natural disaster to crash into Nepal since the 1934 Nepal–Bihar earthquake. Gorkha earthquake was occurred on April 25, 2015 at 11:56 NST and killed more than 10,000 people and injured more than 23,000 population. Its epicentre was east of the district of Lamjung, and its hypocentre was with approximately depth of 15 km with maximum magnitude of 8.1 M_w. Consequently, within 15 to 20 minutes, aftershock was struck across Nepal with a magnitude of 6.7 on 26 April at 12:54:08 NST. Thus, the epicentre of a foremost aftershock was close to the Chinese border between the capital of Kathmandu and Mountain (Figure 1) of Everest with a moment magnitude of 7.3 M_w (Rajghatta, 2015).

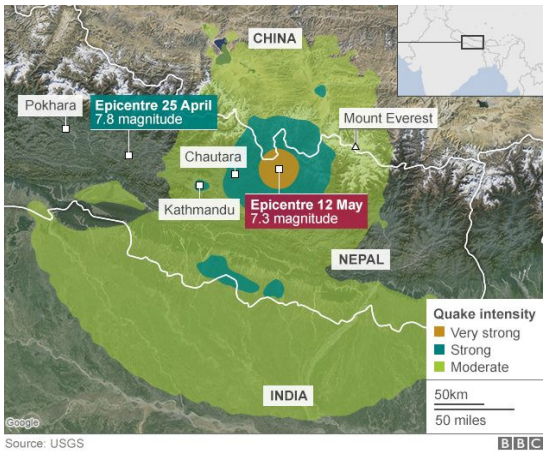

Figure 1. Location of Nepal's earthquake.

Consistent with the USGS (2015), the temblor was caused by a sudden thrust, or release of built-up stress, along the major fault line where the Indian Plate, carrying India, is slowly diving underneath the Eurasian Plate, carrying much of Europe and Asia. Kathmandu, situated on a block of crust approximately 120 km wide and 60 km long, reportedly shifted 3 m to the south in just 30 seconds. Counter to Mughier et al., (2011), Nepal be situated towards the southern limit of the diffuse collisional boundary where the Indian Plate under thrusts the Eurasian Plate, conquering the central district of the Himalayan arc (Figure 2), nearly one-third of the 2,400 km long Himalayas. Geologically, the Nepal Himalayas are partitioned into five tectonic zones from north to south, east to west and approximately equivalent to sub-parallel. Consequently, these five discrete morpho-geotectonic zones are: (1) Terai Plain, (2) Sub Himalaya (Sivalik Range), (3) Lesser Himalaya (Mahabharat Range and mid valleys), (4) Higher Himalaya, and (5) Inner Himalaya (Tibetan Tethys). Each of these zones is obviously identified by their morphological, geological, and tectonic features ((Bollinger et al., 2014). In central Nepal, the convergence rate between the plates is about 45 mm/year. According to USGS (2015), the location, magnitude, and focal mechanism of the earthquake indicate that it was triggered off by a slip along the Main Frontal Thrust (Figure 3).

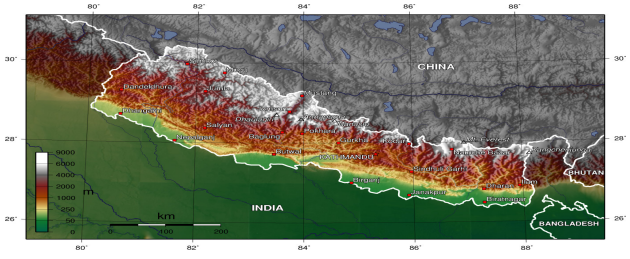

Figure 2. Topography map of Nepal.

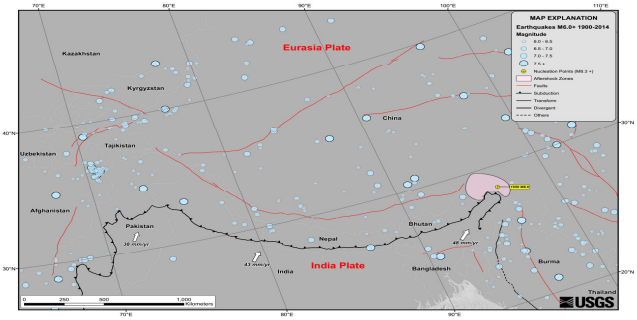

Figure 3. Nepal Himalayas are partitioned into five tectonic zones.

Ravilious (2015) stated that the latest quake follows the same pattern as a duo of big tremors that occurred over 700 years ago, and results from a domino effect of strain transferring along the fault. The last time the fault ruptured at this location was back in 1344. It was preceded in 1255 by a big event to the east of Kathmandu. The last rupture there was in 1934, hinting strain might accumulate westward. This means that 2015's quake follows the pattern with a gap between events of 80 years or so. On other words, the main Frontal Thrust, on average a great earthquake occurs every 750 ± 140 and 870 ± 350 years in the east Nepal region (Marghany 2015).

3. HYBRID GENETIC ALGORITHM FOUR-DIMENSIONAL PHASE UNWRAPPING

Unwrapping a three-dimensional (3-D) phase volume by any of the prevailing 2-D approaches which involves rectification of the consequential phase offset. Nevertheless, phase unwrapping procedures can be improved by using 3-D as stated by Hussien et al., (2005). Consequently, Marghany (2015) has examined 3-D phase unwrapping and confirmed that decorrelation problems can be solved accurately. Conversely, there is few work on the 3-D phase unwrapping problem (Hussien et al., 2005 and Hooper and Zebker 2007). The 3-D phase unwrapping technique involves of the subsequent phases. First, residues are recognised in the phase volume, and the sort, mark and position of individually residue which are collected. Second, the residues which are sorted to establish loops. Though, rests commonly develop locked loops. Subsequently completely loops are known and locked, the branch surface for respectively is conventional shrinking the loop towards its geometric centre. In this procedure, signposts are construct to specify that the replaced segments constituted a forbidden unwrapping path. The unwrapping is approved by a flood fill algorithm as soon as all the signposts indicating where the branch surfaces are positioned (Hussien et al., 2005).

The 4-D unwrapping is constructed by using the temporal phase unwrapping technique with velocity of ground motion which is encoding instead of time as the unwrapping direction. This approach makes use of four dimensions: x, y, t and V. Each voxel (x, y, t) is unwrapped independently of the rest of the voxels using the velocity encoding dimension. Following Karout (2007), the HGA algorithm relies on estimating the parameters of an n^{th} order-polynomial to approximate the unwrapped surface solution from the wrapped phase data. The coefficients of the polynomial that best unwrap the wrapped phase map are obtained by initial solution of GA algorithm to avoid long time to converge to the global optimum solution. In this context, GA minimizes minimum 4-DBPASL and $Q_{i,j,k,V}$ errors between the gradient of the polynomial unwrapped surface solution and the gradient of the original wrapped phase map. On other words, more precision and lower minimum 3DBPASL and $Q_{i,j,k}$ errors are achieved by increasing the order of the polynomial. This proposed algorithm is mainly applicable to adjoining phase distributions (albeit with gaps). Any optimization problem using a GA requires the problem to be coded into GA syntax form, which is the chromosome form. In this problem, the chromosome consists of a number of genes where every gene correspond to a coefficient in the n^{th}-order surface fitting polynomial as described into equation (2) .

$$f := n \rightarrow \sum_{V}^{n} \sum_{k=0}^{n} \sum_{j=0}^{n} \sum_{i=0}^{n} a_{i,j,k} \hat{\phi}_0^{\,i} \hat{\phi}_0^{\,j} \hat{\phi}_0^{\,k} \hat{\phi}_0^{\,V} \qquad (1)$$

where $a[0....n]$ are the parameter coefficients which are retrieved by the genetic algorithm to approximated the unwrapped phase that can achieve the minimum 4DBPASL and $Q_{i,j,k,V}$ errors. Further, *i,j, kand V* are indices of the pixel location in the unwrapped phase respectively, *n* is the number of coefficients (Hussien et al., 2005).

The initial population is generated by creating an initial solution using one of the Quality guided phase unwrapping algorithm (BPASL algorithm) (Hussien et al., 2005). Following Karout (2007), the initial solution is approximated using a 'polynomial Surface-fitting weighted least-square multiple regression' method. The initial population is then generated based on the initial solution. In doing so, every a_g in each chromosome in the population, a small number relying on the accuracy of the gene that is added or subtracted to the value of the gene as given by,

$$a_g = a_g + (\pm 1)\{10^{[\log(a_g)+\Re]}\} \quad (2)$$

where a_g is the coefficient parameter stored in gene *g*, and $\Re$ is a random number generated between the values.

The accurate 4-D phase unwrapping is obtained by modification of phase matching algorithm proposed by Schwarz (2004). According to Schwarz (2004), phase matching algorithm is matched the phase of wrapped phase with unwrapped phase by the given equation

$$\psi_{i,j,k,V} = \phi_{i,j,k,V} + 2\pi\rho\left[\frac{1}{2\pi}\left(\hat{\phi}_{i,j,k,V} - \phi_{i,j,k,V}\right)\right] \quad (3)$$

Where $\psi_{i,j,k,V}$ is the phase matched unwrapped phase, *i,j, k and V* are the pixel positions in the quality phase map, $\phi_{i,j,k,V}$ is the given wrapped phase, $\hat{\phi}_{i,j,k,V}$ is the approximated unwrapped phase, $\rho[.]$ is a rounding function which is defined by $\rho[t] = \lfloor t + 1/2 \rfloor$ for $t \geq 0$ and $\rho[t] = \lfloor t - 1/2 \rfloor$ for $t < 0$ and are *i,j ,k and V* the pixel positions in *x* and *y,z,t* directions, respectively. Phase unwrapping in Equation 3 can be extended to four-dimension to

$$\sum_{i,j,k,V} w^{x}_{i,j,k,V} \left|\Delta\phi^{x}_{i,j,k,V} - \Delta\psi^{x}_{i,j,k,V}\right|^{P} + \sum_{i,j,k,V} w^{y}_{i,j,k,V} \left|\Delta\phi^{y}_{i,j,k,V} - \Delta\psi^{y}_{i,j,k,V}\right|^{P} + \sum_{i,j,k,V} w^{z}_{i,j,k,V} \left|\Delta\phi^{z}_{i,j,k,V} - \Delta\psi^{z}_{i,j,k,V}\right|^{P} + \sum_{i,j,k,V} w^{t}_{i,j,k},V \left|\Delta\phi^{t}_{i,j,k,V} - \Delta\psi^{t}_{i,j,k,V}\right|^{P} \quad (4)$$

where $\Delta\phi$ and $\Delta\psi$ are the unwrapped and wrapped phase differences in *x,y,z,t* respectively, and w represents user-defined weights. The summations are carried out in both *x ,y,z,t* directions over all *i,j ,k and V*, respectively. Then the phase unwrapping based on the quality map can be modified to 4-D as (Marghany 2015),

$$Q_{m,n,l,t} = \frac{1}{m\times n\times lxt} * ((\sum(\Delta\phi^{x}_{i,j,k,V} - \overline{\Delta\phi^{x}_{i,j,k,V}})^2)^{0.5} + ((\sum(\Delta\phi^{y}_{i,j,k,V} - \overline{\Delta\phi^{y}_{i,j,k,V}})^2)^{0.5} + ((\sum(\Delta\phi^{z}_{i,j,k,V} - \overline{\Delta\phi^{z}_{i,j,k,t}})^2)^{0.5} + ((\sum(\Delta\phi^{t}_{i,j,k,V} - \overline{\Delta\phi^{t}_{i,j,k,t}})^2)^{0.5}, \quad (5)$$

where $\Delta\phi^{x}, \Delta\phi^{y}, \Delta\phi^{z}$ and $\Delta\phi^{t}$ are the unwrapped-phase gradients in the *x*, *y*, *z, and t* directions, respectively. $\overline{\Delta\phi}^{x}, \overline{\Delta\phi}^{y}, \overline{\Delta\phi}^{z}$ and $\overline{\Delta\phi}^{t}$ are the mean of unwrapped-phase gradient in $m\times n\times lxt$ cube in $\Delta\phi^{x}, \Delta\phi^{y}, \Delta\phi^{z}$ and $\Delta\phi^{t}$, respectively. *i,j,k,*and *t* are neighbours' indices of the voxel *v*_in *m*, *n*, *l* and *t*.

4. RESULTS AND DISCUSSION

Figure 4 shows the Sential-1A data were acquired pre-earthquake and post-earthquake on April 17 and 29 2015, respectively. The urban zones and top of mountains are dominated with higher coherence of 0.8 and 1 respectively as compared to vegetation and water. On contrast, The water has lower backscatter and coherence of -30 dB and 0.25, respectively (Figure 4b). In fact, Sential-1A beam mode of interferometric wide swath has spatial resolution of 5 x 20 m and swath width of 250 km with VV polarization.

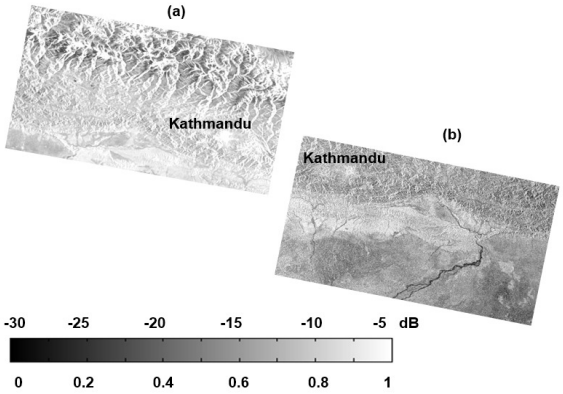

Figure 4. Sential-1 A satellite data (a) pre and (b) post earthquake.

Figure 5 shows the interfergram produced by ESA (2015) by combining two Sentinel-1A radar scans from 17 and 29 April 2015. This interferogram shows changes on the ground that occurred during the 25 April earthquake that struck Nepal. An overall area of 120x100 km has moved – half of that uplifted and the other half, north of Kathmandu subsided. Vertical accuracy is a few cm (ESA 2015). Additional, each 'fringe' of colour represents about 3 cm of deformation. The large amount of fringe indicates a large deformation pattern with ground motions of 1 m or more. Sentinel-1A interferogram over Kathmandu, Nepal shows deformation induced by the 25 April 2015 earthquake. East–west 'fringes' cross the city, with each coloured fringe corresponding to 2.8 cm of ground displacement (both uplift and subsidence) (Marghany 2015).

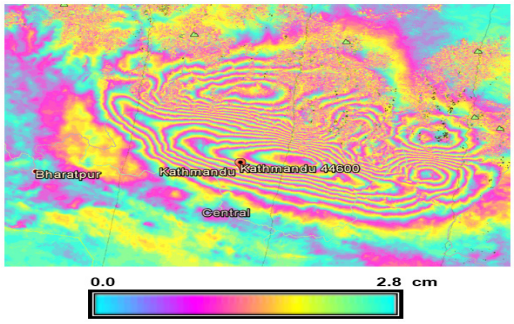

Figure 5. Sentinel-1A interferogram over Kathmandu produced by ESA (2015)

The interferogram fringes produced by using the combination of four-dimensional best-path avoiding singularity loops (4DBPASL) algorithm and HGA algorithm. Clearly, the proposed algorithm for 4-D phase unwrapping produced vibrant fringe cycles which indicate critical surface motion of 8.5 cm which is coincided with ground motion of 1.4 m north of Kathmandu (Figure 6). In fact, the 4DBPASL algorithm acquires an optimal unwrapping path, whereas it is also taking into account the effect of singularity loops. In addition, zero-weighted edge is used zero-weighted edges to adjust the optimal path and avoid these singularity loops. With this regard, 4-D 4DBPASL interferometry fringes produced by using Hybrid Genetic Algorithm. It is interesting to find that the proposed algorithm has produced clear fringe patterns. In fact, the proposed algorithm has minimized the error in interferogram cycle due decorrelation effects. This could be improvement of such previous work of Hussein et al. (2005); Karout(2007);Marghany (2015).

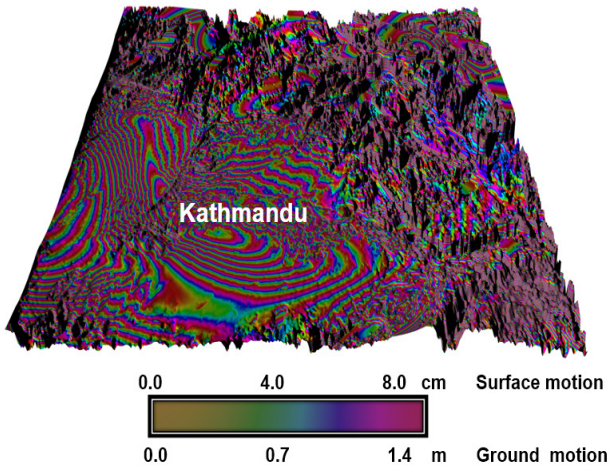

Figure 6. Interferometry produced by Hybrid Genetic Algorithm for 4-DBPASL .

In line with Hussien et al., (2005),the 4DBPASL not only identifies these singularity loops, but it also calculates the quality of each voxel to ensure that the most reliable voxels are unwrapped first and thus the effects of singularity loop ambiguities are minimized or removed entirely. Consequently, the combination of 4DBPASL for phase unwrapping with hybrid Genetic algorithm produced more precisely fringe cycle. With this regard, hybrid Genetic algorithm matches the phase of the wrapped phase with approximated unwrapped phase to establish the best representation of the unwrapped phase and displacement deformation.

5. CONCLUSIONS

This study has demonstrated new approach for 4-D phase unwrapping based on Hybrid Genetic algorithm for four-dimensional Nepal ‘s earthquake study. In doing so, Sential-1 A satellite data beam mode of interferometric wide swath during April 17 and 29 April 2015. Additional, four -dimensional phase unwrapping is performed using modification of three-dimensional best-path avoiding singularity loops (3DBPASL) algorithm. Then phase matching is implemented with 4-DBPASL using Hybrid Genetic Algorithm (GHA). The study shows that the surface motion of 8.5 cm which is coincided with ground motion of 1.4 m north of Kathmandu. In conclusion, integration of the GHA with 4DBPASL phase unwrapping produce excellent 4-D Nepal ‘s earthquake surface displacement using Sential-1 A satellite data beam mode of interferometric.

References

Bollinger, L., S. N. Sapkota, P. Tapponnier, Y. Klinger, M. Rizza, J. Van der Woerd, D. R. Tiwari, R. Pandey, A. Bitri, S. Bes de Berc (2014). "Return period of great Himalayan earthquakes in Eastern Nepal: evidence from the Patu and Bardibas strands of the Main Frontal Thrust". *Journal of Geophysical Research*.

ESA 2015. Nepal earthquake on the radar.
https://sentinel.esa.int/web/sentinel/news/-/article/nepal-earthquake-on-the-radar. [Access August 20, 2015].

Hai Li and Renbiao W. (2012) Robust Interferometric Phase Estimation in InSAR via Joint Subspace Projection. In Padron I. (ed.) "Recent Interferometry Applications in Topography and Astronomy". InTech - Open Access Publisher, University Campus STeP Ri, Croatia. (2012), 111-132.

Hussein S A, Gdeist M, Burton D, Lalor M., 2005 Fast three-dimensional phase unwrapping algorithm based on sorting by reliability following a *non-continuous path Proc. SPIE*, **5856** 40.

Haupt R L, and Haupt S E 2004. Practical genetic algorithms , John-Wiley & Sons.

Hooper, A. and Zebker, H.A., 2007. Phase unwrapping in three dimensions with application to InSAR time series. *JOSA A*, *24*(9), pp.2737-2747.

Karout S., 2007., Two-Dimensional Phase Unwrapping, Ph.D Theses, Liverpool John Moores University , 2007.

Marghany M., 2012. Simulation of 3-D Coastal Spit Geomorphology Using Differential Synthetic Aperture

Interferometry (DInSAR). In I. Padron.,(ed.) Recent Interferometry Applications in Topography and Astronomy. Croatia: InTech – Open Access Publisher, (2012) 83-94.

Marghany M. 2013. DInSAR technique for three-dimensional coastal spit simulation from radarsat-1 fine mode data. Acta Geophysica .61,2, 478-493.

Marghany M. 2014a. Simulation of three-dimensional of coastal erosion using differential interferometric synthetic aperture radar, Global NEST Journal, Vol 16, No 1, pp 80-86.

Marghany, M. 2014b. Hybrid Genetic Algorithm of Interferometric Synthetic Aperture Radar For Three-Dimensional Coastal Deformation. *Frontiers in artificial intelligence and applications: new trends in software methodologies, tools and technique*, *265*, 116-31.

Marghany M., 2015, Fourth dimensional optical hologram interferometry of RapidEye for Japan ‘s tsunami effects” CD of 36th Asian Conference on Remote Sensing (ACRS 2015), Manila, Philippines, 24-28 October 2015, http://www.a-a-r-s.org/acrs/index.php/acrs/acrs-overview/proceedings-1?view=publication&ta=show&id=1691.

Mughier J.L., Huyghe P., Gajurel A.P., Upreti B.N. and Jouanne F.; Huyghe; Gajurel; Upreti; Jouanne (2011). "Seismites in the Kathmandu basin and seismic hazard in central Himalaya"(PDF). *Tectonophysics* **509** (1–2): 33–49.

Pepe A. 2012. Advanced Multitemporal Phase Unwrapping Techniques for DInSAR Analyses. In Padron I. (ed.) "Recent Interferometry Applications in Topography and Astronomy". InTech - Open Access Publisher, University Campus STeP Ri, Croatia. (2012),57-82.

Saravana, S.S., Ponnanbalam, S.G., Rajendran, C. A. 2003. Multi-objective genetic algorithm for scheduling a flexible manufacturing system, *International Journal of Advanced Manufacturing Technology*, **22**, 229-236.

Schwarz O. 2004. Hybrid phase unwrapping in laser speckle interferometry with overlapping windows, Shaker Verlag.

Rajghatta C., 2015. "Is this the 'Big Himalayan Quake' we feared?". *The Time of India*. Retrieved 26 April 2015.

Ravilious K. 2015.Nepal quake “followed historical pattern” http://www.bbc.com/news/science-environment-32472310. [Access on August 19 2015].

USGS 2015. Himalayan Tectonic. http://earthquake.usgs.gov/earthquakes/tectonic/images/himalaya_tsum.pdf. [Acess on August 19 2015].

Zebker H.A. , P.A. Rosen, and Hensley S. 1997. Atmospheric effects in inteferometric synthetic aperture radar surface deformation and topographic maps. *J. Geophys. Res.***102**, 7547-7563.